J BONE ONCOL 47 (2024) 100625

Contents lists available at ScienceDirect

Journal of Bone Oncology

journal homepage: www.elsevier.com/locate/jbo

Research Paper

Pharmacologic Hedgehog inhibition modulates the cytokine profile of osteolytic breast cancer cells

Natalie E. Bennett [a,b,c,d], Dominique V. Parker [a,b,c], Rachel S. Mangano [b,c,e], Jennifer E. Baum [b,c,f], Logan A. Northcutt [a,b,c], Jade S. Miller [b,c,g], Erik P. Beadle [b,c,h], Julie A. Rhoades [a,b,c,h,i,*]

[a] Program in Cancer Biology, Vanderbilt University, Nashville, TN, United States
[b] Center for Bone Biology, Vanderbilt University Medical Center, Nashville, TN, United States
[c] United States Department of Veterans Affairs, Tennessee Valley Healthcare System, Nashville, TN, United States
[d] Medical Scientist Training Program, Vanderbilt University, Nashville, TN, United States
[e] Interdisciplinary Graduate Program in Biological and Biomedical Sciences, Vanderbilt University, Nashville, TN, United States
[f] Master's Program in Biomedical Sciences, Vanderbilt University, Nashville, TN, United States
[g] Pharmacology Training Program, Department of Pharmacology, Vanderbilt University, Nashville, TN, United States
[h] Division of Clinical Pharmacology, Department of Medicine, Vanderbilt University Medical Center, Nashville, TN, United States
[i] Department of Biomedical Engineering, Vanderbilt University, Nashville, TN, United States

HIGHLIGHTS

- Gli2 correlates with myeloid gene signatures in sequencing data of patient tumors.
- HPI-1 treatment alters transcription and secretion of cytokines, including M−CSF.
- This altered secretory profile induces a proinflammatory phenotype in monocytes.

ARTICLE INFO

Keywords:
Breast cancer
Bone metastasis
Monocyte
Myeloid
Cytokine
M−CSF

ABSTRACT

The establishment and progression of bone metastatic breast cancer is supported by immunosuppressive myeloid populations that enable tumor growth by dampening the innate and adaptive immune response. Much work remains to understand how to target these tumor-myeloid interactions to improve treatment outcomes. Non-canonical Hedgehog signaling is an essential component of bone metastatic tumor progression, and prior literature suggests a potential role for Hedgehog signaling and its downstream effector Gli2 in modulating immune responses. In this work, we sought to identify if inhibition of noncanonical Hedgehog signaling alters the cytokine profile of osteolytic breast cancer cells and the subsequent communication between the tumor cells and myeloid cells. Examination of large patient databases revealed significant relationships between Gli2 expression and expression of markers of myeloid maturation and activation as well as cytokine expression. We found that treatment with HPI-1 reduced tumor cell expression of numerous cytokine genes, including *CSF1*, *CSF2*, and *CSF3*, as well as *CCL2* and *IL6*. Secreted CSF-1 (M−CSF) was also reduced by treatment. Changes in tumor-secreted factors resulted in polarization of THP-1 monocytes toward a proinflammatory phenotype, characterized by increased CD14 and CD40 surface marker expression. We therefore propose M−CSF as a novel target of Hedgehog inhibition with potential future applications in altering the immune microenvironment in addition to its known roles in reducing tumor-induced bone disease.

1. Introduction

Metastasis of cancer cells to distant sites is a leading cause of morbidity and mortality among patients with breast cancer. Although outcomes have improved in recent decades, patients with metastatic disease at the time of breast cancer diagnosis have a 21% five-year

* Corresponding author.
E-mail address: julie.rhoades@vumc.org (J.A. Rhoades).

https://doi.org/10.1016/j.jbo.2024.100625
Received 6 May 2024; Received in revised form 23 July 2024; Accepted 24 July 2024
Available online 28 July 2024
2212-1374/© 2024 The Authors. Published by Elsevier GmbH. This is an open access article under the CC BY-NC-ND license (http://creativecommons.org/licenses/by-nc-nd/4.0/).

survival rate[1]. Bone is the most common site of breast cancer metastasis among most subtypes[2]. In fact, in patients diagnosed with Stage IV breast cancer, over 50% have evidence of bone metastases at the time of diagnosis[3]. Anti-resorptive medications, such as bisphosphonates and receptor activator of nuclear factor-κB ligand (RANKL) inhibitors, are a mainstay of treatment for patients with bone metastases for reducing morbidity associated with bone destruction[4]. However, bone metastasis is considered to have no cure[5], emphasizing the importance of understanding the unique interactions within the bone microenvironment between tumor cells and neighboring populations.

Over half of patients with bone metastases experience skeletal-related events (SREs), such as bone pain, fracture, and spinal cord compression[6,7]. This is due to tumor-induced bone disease (TIBD) caused by aberrant regulation of homeostatic bone remodeling processes. The osteolytic lesions characteristic of bone metastatic breast cancer result from tumor cell secretion of parathyroid hormone-related protein (PTHrP), which is regulated by the transcription factor Gli2, inducing osteolytic bone destruction and tumor growth[8]. This transcription factor is overexpressed in breast cancer bone metastases[9]. While Gli2 is canonically a downstream effector of the Hedgehog pathway, which is important in limb and skeletal development[10], its actions in bone metastatic breast cancer are via a noncanonical mechanism in which Gli2-mediated PTHrP expression is driven by TGF-β signaling through TGF-β receptor type II[11] and SMAD activation[12]. This is further supported by a pan-cancer patient data analysis demonstrating that in Gli-expressing tumors, Gli expression is more closely correlated to TGF-β genes than canonical Hedgehog signaling genes[13]. This cycle feeds back upon itself as TGF-β plays a direct transcriptional role in increasing Gli2 expression by binding a TGF-β-responsive sequence in the Gli2 promoter[14]. Targeting this noncanonical Hedgehog pathway by inhibiting Gli2 has therapeutic benefit in reducing TIBD, using both genetic[11,15]and drug[9,16] targeting strategies.

Despite the fundamental importance of Gli2 and noncanonical Hedgehog signaling in the growth of bone metastases, there has been little work studying its role in the crosstalk between tumor cells and other cells in the bone microenvironment. However, recent studies have demonstrated the potential role of Gli2 in modulating the immune microenvironment. For example, Gli2 activation is associated with an increase in IL-4, IL-6, IL-10, and TGF-β[17–20]. In fact, Gli2 has been shown to bind the promoter for IL-6[20] and an enhancer site for IL-4 [17]. A recent study in pancreatic cancer demonstrated that fibroblast Gli2/Gli3 knockout results in differential cytokine expression, leading to a reduction in tumor-supportive myeloid-derived suppressor cells (MDSCs) and mature immunosuppressive macrophages[21]. These processes are of particular interest in bone metastatic breast cancer, given the importance of Gli2 and noncanonical Hedgehog signaling in driving disease. Work from our lab and others has demonstrated that MDSCs[22,23] and tumor-infiltrating macrophages[24] are important for the establishment and outgrowth of bone metastatic breast cancer. This work underscores the potential of using Gli2 and noncanonical Hedgehog inhibition as an avenue for modifying tumor cell-myeloid relationships.

In this study, we hypothesized that inhibition of noncanonical Hedgehog signaling modifies cytokine expression by osteolytic breast cancer cells, thereby altering tumor cell-myeloid cell interactions. We evaluated this hypothesis through multiple approaches, including bioinformatic analysis of patient datasets, gene expression and cytokine assays, and *in vitro* assays of myeloid response to drug-treated tumor cells. Identification of novel roles of Gli2 and Hedgehog signaling in tumor microenvironmental interactions can provide key insights for future preclinical and clinical studies targeting this niche.

2. Material and methods

2.1. Bioinformatic analysis

Publicly available bulk RNA sequencing and protein expression data of patient tumors from the Cancer Genome Atlas (TCGA) – Breast Invasive Carcinoma cohort (n = 1053) was accessed and visualized through cBioPortal[25–27]. Co-expression analyses were performed using cBioPortal, and the Spearman's correlation of mRNA expression of key myeloid lineage phenotypic markers versus Gli2 mRNA expression was calculated. Then, samples were stratified into quartiles based on level of Gli2 mRNA expression (mRNA expression, RSEM, batch normalized from Illumina HiSeq_RNASeqV2). Subsequent analyses of TCGA data utilized the top quartile (Gli2 high, mean log2 expression of 121.83–571.31, n = 271) and bottom quartile (Gli2 low, 0.79–37.67, n = 270). A list of 430 genes related to myeloid differentiation and activation was compiled based on the following Gene Ontology lists[28–30] (filtered for human genes, excluded NOT terms, and removed duplicate genes): GO:0002275 (myeloid cell activation involved in immune response), GO:0002444 (myeloid leukocyte mediated immunity), GO:0002274 (myeloid leukocyte activation), GO:0030099 (myeloid cell differentiation). Significant differences of these genes between the Gli2-high and Gli2-low groups were calculated using the Student's *t*-test with FDR correction for multiple comparisons. Differences in expression of cytokine genes and ESR1 expression were similarly calculated. Expression data of Gli2 across major breast cancer subtypes was also obtained, with TCGA-normal (normal-like tumor tissue) excluded. Additionally, data of protein levels measured via reverse-phase protein array (RPPA) was obtained from TCGA, and estrogen receptor 1 protein expression in Gli2-low and Gli2-high tumors was evaluated. The Human Protein Atlas (https://www.proteinatlas.org)[31] was also queried for Gli2, and information about its expression in immune populations was accessed. Additionally, further bulk RNA sequencing data was obtained from The Metastatic Breast Cancer Project (https://www.mbcproject.org/) [32,33], also via cBioPortal, and Spearman's correlation of mRNA expression of key myeloid lineage phenotypic markers and CSF1/CSF1R versus Gli2 mRNA expression was calculated. Finally, mRNA expression data of Gli2 and other Hedgehog signaling components in laboratory breast cancer cell lines and THP-1 cells was collected via the Cancer Cell Line Encyclopedia (CCLE)[34] (accessed via cBioPortal and the Broad Institute CCLE portal itself). Breast cancer lines were selected by filtering for lines marked with the cancer type "Breast Cancer" that had mRNA expression data available and removing five fibroblast lines from the resultant list. For analyses comparing Gli2 between ER-negative and ER-positive cell lines, outliers were removed using the ROUT method.

2.2. Cell culture

The human breast cancer cell line MDA-MB-231 was obtained from American Type Culture Collection (ATCC), and a bone-metastatic variant (MDA-MB-231b) was generated as previously described [9,11,35–37]. Cells were maintained in DMEM (high glucose, pyruvate; Gibco) supplemented with 10% fetal bovine serum (FBS; Peak Serum) and 1% penicillin/streptomycin (Corning). The human breast cancer cell line MDA-MB-436 was also obtained from ATCC and maintained using the same culture conditions as MDA-MB-231b cells. The human monocytic cell line THP-1 was obtained from ATCC and maintained in RPMI 1640 (Corning) with 10% FBS and 1% penicillin/streptomycin.

2.3. Drug treatments on breast cancer cells

MDA-MB-231b were plated in 6-well plates at a seeding density of 70,000 cells per well and allowed to adhere overnight in DMEM with 10% FBS and 1% penicillin/streptomycin. The following day, media was changed to serum-free DMEM for 8 hours (h) prior to initiation of drug treatment. Human recombinant TGF-β1 (R&D Systems) and Hedgehog

Pathway Inhibitor 1 (HPI-1; Tocris) were reconstituted in sterile filtered 4 mM HCl with 1 mg/ml bovine serum albumin (Sigma-Aldrich) or DMSO (Sigma-Aldrich), respectively. Cells were treated with TGF-β1 with or without HPI-1 in the following groups: 5 ng/ml TGF-β1, 5 ng/ml TGF-β1 + 1 μM HPI-1, 5 ng/ml TGF-β1 + 5 μM HPI-1, and vehicle control for 24 or 48 hours. MDA-MB-436 cells were treated with 5 ng/ml TGF-β1 or 5 ng/ml TGF-β1 + 5 μM HPI-1 using the same protocol with an original seeding density of 150,000 cells per well.

2.4. RNA extraction and Quantitative Real-Time PCR

RNA from drug-treated breast cancer cells was collected using phenol (QIAzol; Qiagen)-chloroform (Fisher Scientific) isolation followed by isopropanol (Sigma-Aldrich) precipitation as per QIAzol manufacturer instructions. Complementary DNA (cDNA) was synthesized from 1 μg RNA using SuperScript VILO Master Mix (Invitrogen). For standalone *PTHLH* expression analysis, studies were performed using TaqMan Universal PCR Master Mix (Applied Biosystems) and TaqMan primers for eukaryotic 18S rRNA (4352930E; Applied Biosystems) and human *PTHLH* (Hs00174969_m1, Thermo Fisher). Quantitative real-time PCR (qRT-PCR) was performed on the QuantStudio 7 Pro Real-Time PCR System (Applied Biosystems) using the following conditions: 2 min at 50°C, 10 min at 95°C, (15 s at 95°C, 1 min at 60°C) × 40 cycles. Gene expression was calculated using the relative quantification method (ddCT) with 18S as an endogenous control.

2.5. Custom TaqMan PCR array

Taqman Array Plates (Thermo Fisher) were custom-ordered with the gene expression assays listed in **Table S1**. cDNA from MDA-MB-231b cells and MDA-MB-436 cells treated with 5 ng/ml TGF-β1 or 5 ng/ml TGF-β1 + 5 μM HPI-1 was used for the arrays. Arrays were run on three biological replicates. cDNA from three technical replicates was pooled for each biological replicate, combined with TaqMan Universal PCR Master Mix, and added to the array plate with 100 ng of cDNA per well (one array plate per biological replicate). qRT-PCR was performed as described above. *18S*, *ACTB*, and *GAPDH* were included on the arrays as potential endogenous controls. Gene expression was calculated using the relative quantification method (ddCT) with 18S as the endogenous control (selected based on lowest variability between groups and within replicates).

2.6. Cytokine protein assays

After 48 h of drug treatments as described above, conditioned media was collected from MDA-MB-231b cells and MDA-MB-436 cells and centrifuged at 1000 x g for 10 min. Supernatant was collected and stored at −80°C until ready to use for cytokine assays. MDA-MB-231b samples were submitted to the VUMC Analytical Services Core for measurement of cytokines from the MILLIPLEX MAP Human Cytokine/Chemokine Magnetic Bead Panel (Millipore Sigma). Total protein concentration was quantified using the Pierce BCA Protein Assay (Thermo Fisher). MDA-MB-231b and MDA-MB-436 conditioned media samples were then used for the M−CSF (CSF-1) Human ELISA Kit (Invitrogen), which was performed per manufacturer instructions.

2.7. Tumor-conditioned media treatments on THP-1 Cells: qRT-PCR

MDA-MB-231b cells were treated with 5 ng/ml TGF-β1 or 5 ng/ml TGF-β1 + 5 μM HPI-1 as described above. Following 48 h of treatment, treatment media was removed, and cells were washed with phosphate buffered saline (Gibco) and cultured in serum-free DMEM for an additional 24 or 48 h. Cell culture media was centrifuged at 1000 x g for 10 min, and supernatant (tumor-conditioned media, TCM) was collected and stored at −80°C until ready for use. THP-1 cells were seeded at 250,000 cells per well in a 12-well dish and treated with a 1:1 ratio of TCM to complete RPMI (with 10% FBS and 1% penicillin–streptomycin) as previously described[38,39]. Cells were incubated for 72 h, and adherent and non-adherent cells were collected in QIAzol for RNA extraction, cDNA synthesis, and qRT-PCR as described above using primers for eukaryotic 18S rRNA and those listed in **Table S2** (Thermo Fisher).

2.8. Tumor-conditioned media treatments on THP-1 Cells: Flow cytometry

THP-1 cells were cultured with 1:1 TCM and RPMI for 3 days as described above or for 5 days with supplementation of an additional 0.5 ml of 1:1 TCM:RPMI at day 3. Adherent cells were detached from wells using Accutase (Sigma-Aldrich) and pooled with nonadherent cells from the same treatment group. 500,000 cells per test were stained for viability with Ghost Dye Violet 510 (Tonbo) at a dilution of 1:5000 followed by Fc receptor blocking using 1 μL per test of Human Trustain FcX (Biolegend). Samples and fluorescence minus one controls were stained using antibodies at dilutions listed in **Table S3**. Single stain controls were prepared using compensation beads (Invitrogen). Samples were fixed with 2% paraformaldehyde, and flow cytometry was performed on the Cytek Aurora spectral flow cytometer (Cytek Biosciences). Analyses were completed using FlowJo software (BD Life Sciences). Experiments were performed three times. Histograms shown are representative and were generated in FlowJo.

2.9. Statistical analysis

All statistical analyses were performed using Prism 10.2.0 (GraphPad Software). Values are presented as mean and standard deviation (SD) unless otherwise noted in figure captions. Analyses with one target were performed using the unpaired *t*-test (*$p < 0.05$). Analyses with more than one gene or protein target were performed by multiple unpaired t-tests with correction for multiple comparisons (FDR, Benjamini-Hochberg procedure, Q=5%, *$q < 0.05$). Finally, analyses with more than two groups were performed using the one-way ANOVA test (*$p < 0.05$). Outlier testing for *in vitro* experiments was performed using ROUT method ($Q < 1\%$). Experiments were performed with three independent biological replicates unless otherwise specified.

3. Results

3.1. Bioinformatic analysis of patient tumors reveals significant correlations between Gli2 and myeloid gene signatures

To explore the clinical validity of our research question, we first sought to identify relationships between Gli2 expression and myeloid markers in patient tumor databases. Large datasets of bone metastatic tumors are limited, so we utilized bulk RNA sequencing data of 1053 primary breast tumors in The Cancer Genome Atlas accessed via cBioPortal[25–27] (workflow in Fig. 1**A**). Gli2 mRNA expression was correlated with a number of key myeloid phenotypic genes, including early myeloid progenitor markers such as *CD33* and *CD34* as well as markers of downstream myeloid differentiation, such as *ITGAM* (CD11b), *CD14*, and *CD15* (Fig. 1**B**). Similar correlations were seen in primary tumor data from patients with known bone metastasis from the Metastatic Breast Cancer Project cohort[32,33] (Fig. 1**C**). Because of these correlations between Gli2 and myeloid phenotypic markers, we then analyzed relationships between Gli2 and markers of myeloid activation and maturation (workflow in Fig. 2**A**). A list of 430 genes was compiled based on four Gene Ontology lists[28–30]: GO:0002275 (myeloid cell activation involved in immune response), GO:0002444 (myeloid leukocyte mediated immunity), GO:0002274 (myeloid leukocyte activation), GO:0030099 (myeloid cell differentiation). Patient samples from TCGA were stratified into Gli2-high tumors (top 25% of Gli2 mRNA expression) and Gli2-low tumors (bottom 25% of Gli2 mRNA

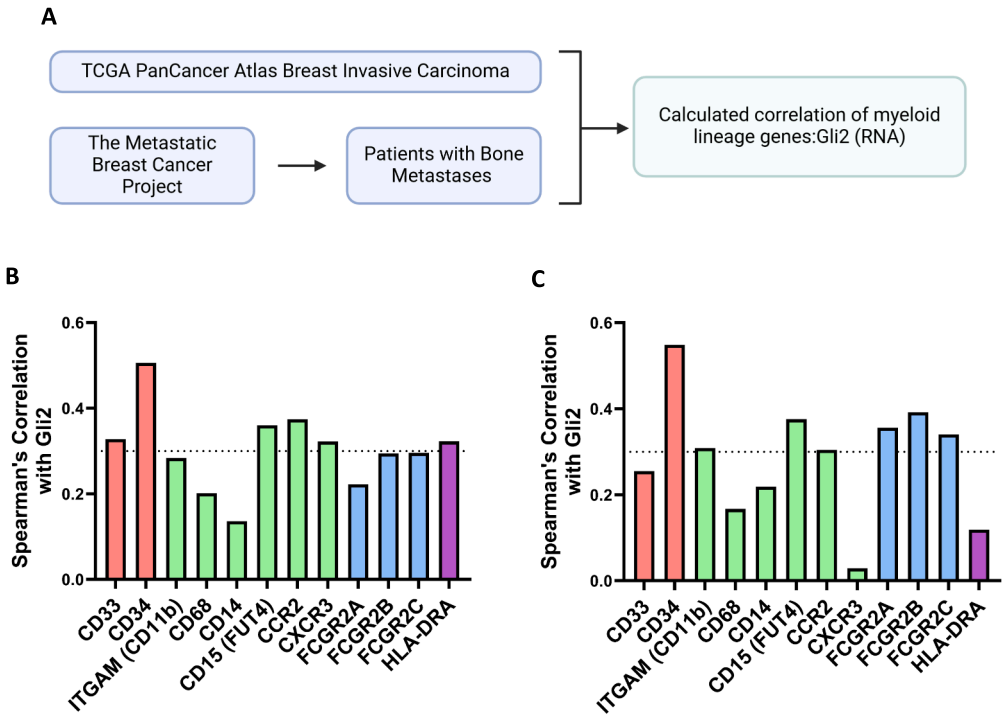

Fig. 1. Patient database analysis reveals correlations between Gli2 and markers of myeloid lineage. Among all breast cancer samples in The Cancer Genome Atlas (TCGA) and among patients with bone metastases in the Metastatic Breast Cancer Project (MBCP), Gli2 is correlated with markers of early myeloid differentiation, such as CD33 and CD34, as well as markers of downstream myeloid subtypes. (A) Flowchart of methods used to analyze patient data from primary breast tumors from TCGA and MBCP (data accessed through cBioPortal). (B) Spearman's correlation between mRNA expression of Gli2 and myeloid phenotypic markers (red = general myeloid lineage, green = myeloid subsets, blue = antibody receptors, purple = antigen presentation) in samples from TCGA. Dashed line at Spearman's coefficient of 0.3 (n = 1053 tumors). (C) Spearman's correlation between mRNA expression of Gli2 and myeloid phenotypic markers in primary tumor samples from patients with bone metastases in MBCP (n = 84 tumors). Schematic created with Biorender.com. (For interpretation of the references to colour in this figure legend, the reader is referred to the web version of this article.)

expression). Of the 430 genes evaluated, 331 were significantly different between Gli2-high and Gli2-low tumors (Fig. 2**B**, top 50 most significant differentially expressed genes from the myeloid gene list shown in **Table S4**). These findings demonstrate a robust relationship between Gli2 and markers of myeloid populations and their activity. Although this could be mediated by a number of mechanisms, we predicted that high Gli2 levels in the tumor may be correlated with cytokine expression. In Gli2-high tumors, there was increased gene expression of *TGFB1/2/3, CSF1/1R, CCL2, CXCL8, IL6,* and *IL10 (*Fig. 2**C**), many of which are important in bone metastasis or recruitment of immunosuppressive myeloid populations[40–42]. Finally, we queried Gli2 through the Human Protein Atlas[31], which demonstrated that Gli2 is not detected in bone marrow or circulating immune cells (data not shown). These are the primary sources of tumor-infiltrating myeloid cells in primary and bone metastatic breast cancer[24,43], suggesting that the correlations between Gli2 and markers of myeloid cells or cytokines are not due to Gli2 in the myeloid cells themselves. Despite the lack of large databases containing sequencing data from breast cancer bone metastases themselves, data from primary tumors shows promising correlations between tumoral Gli2 levels and myeloid populations, supporting the validity of exploration at the bench. Differences in cytokines in Gli2 high versus low tumors suggest a potential mechanism that is explored *in vitro* in subsequent experiments.

3.2. Hedgehog pathway inhibitor treatment modifies cytokine gene expression in osteolytic breast cancer cells

To better understand the Gli2-myeloid relationships seen in patient tumor data, we proceeded with *in vitro* experiments utilizing a small-molecule inhibitor of the Hedgehog pathway (Hedgehog pathway inhibitor 1, HPI-1) to inhibit Gli2-mediated signaling. In patient data, Gli2 is expressed across the major breast cancer subtypes (Fig. 3**A**), with basal tumors having higher Gli2 expression than Luminal B and Her2 tumors. Among all breast tumor subtypes, ESR1 (estrogen receptor 1) mRNA and protein expression are higher in tumors in the bottom quartile of Gli2 expression than tumors in the top quartile (Fig. 3**B-C**). Similarly, among breast cancer cell lines used in the laboratory, estrogen receptor (ER)-negative cell lines express significantly higher Gli2 than ER-positive cell lines (Fig. 3**D**), aligning with prior work showing that non-osteolytic cell lines are Gli2-negative and often ER-positive[8]. Because of the limited availability of osteolytic breast cancer lines that express both Gli2 and ER, we proceeded with *in vitro* experiments using two triple-negative cell lines: a bone metastatic variant of the human breast cancer cell line MDA-MB-231 (MDA-MB-231b), which is well-established in our lab, and MDA-MB-436 cells, which are also known to have osteolytic capacity[35]. HPI-1 inhibits Hedgehog signaling by blocking the activity of the Gli transcription factors downstream of Sonic Hedgehog ligand or Smoothened[44]. As described above, Hedgehog signaling in bone metastatic breast cancer cells occurs through a non-canonical route, bypassing Smoothened and signaling through TGF-β-driven activation of Gli2[11]. Common osteolytic cell lines used in research do not express Smoothened and have lower expression of Patched than non-osteolytic cell lines, and Gli2 (but not Gli1 and Gli3) drives expression of PTHrP, a central mediator of TIBD[8,11]. Therefore, HPI-1 can be used to block noncanonical Hedgehog signaling in these breast cancer cells.

To identify the optimal dosing strategy, MDA-MB-231b cells were treated for 24 and 48 h with TGF-β and increasing doses of HPI-1, and qRT-PCR analysis demonstrated that TGF-β increased *PTHLH* expression (gene name for PTHrP), and 1 μM and 5 μM HPI-1 treatment for 48 h

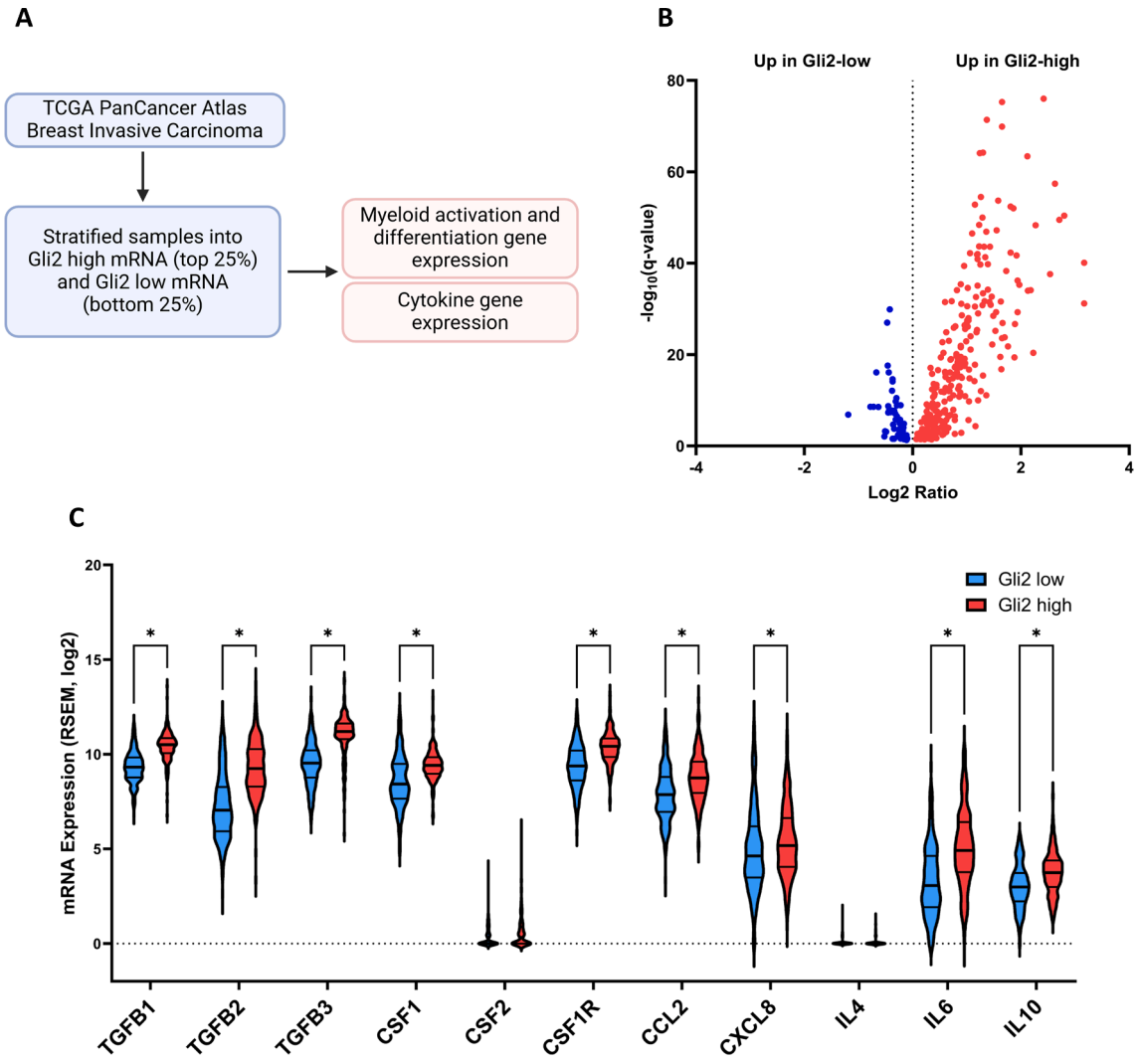

Fig. 2. Gli2-high tumors have increased expression of myeloid activation and differentiation genes and cytokines important in bone metastasis. (A) Flowchart of methods used to analyze patient data from primary breast tumors from The Cancer Genome Atlas (TCGA) PanCancer Atlas (data accessed through cBioPortal). (B) Volcano plot showing mRNA expression of myeloid activation and differentiation genes in tumors with high Gli2 gene expression (top quartile, n = 271 tumors) compared to tumors with low Gli2 gene expression (bottom quartile, n = 270 tumors). Top 50 most significant differentially expressed genes from this list shown in **Table S4**. (C) mRNA expression of cytokines in Gli2 high tumors and Gli2 low tumors. Student's *t* test with FDR correction for multiple comparisons. *q < 0.05. Schematic created in Biorender.com.

reduced PTHLH below baseline (**Figure S1**). Therefore, for subsequent studies, we utilized TGF-β stimulation for all groups due to its relevance to the bone metastatic microenvironment, in which its release from the bone matrix stimulates tumor cell proliferation and increased osteolysis [45]. Additionally, TGF-β itself increases Gli2 transcription[14], further propagating bone metastatic disease, so inclusion of TGF-β in the media of treatment groups is physiologically relevant to the typical microenvironment of osteolytic tumors. The HPI-1 dose selected was 5 μM, which is near the IC50 for inhibition of Gli2-mediated Hedgehog signaling while remaining sub-cytotoxic[44,46], and TGF-β + HPI-1 treatment was compared to TGF-β + vehicle control.

We treated TGF-β-stimulated MDA-MB-231b cells for 48 h with or without 5 μM HPI-1 and performed a PCR array for key genes associated with Hedgehog signaling and tumor-immune interactions (Fig. 4). Genes that were downregulated and upregulated due to HPI-1 treatment are shown in Fig. 4**A and 4B**, respectively. As confirmation of HPI-1 reducing noncanonical Hedgehog signaling, *PTHLH* expression decreased in all replicates (Fig. 4**A**). *GLI2* and *PTCH1* did not change, but *TGFBR2* significantly decreased. *SMO* was not expressed in either treatment group, as expected (**Table S5**).

Gene expression of numerous cytokines and chemokines significantly changed upon HPI-1 treatment. *CCL2*, *IL1B*, *IL6*, and *IL23A* decreased (Fig. 4**A**), whereas *CXCL8*, *IL11*, and *TNF* increased (Fig. 4**B**). Notably, gene expression of all three colony stimulating factors (*CSF1*, *CSF2*, and *CSF3*) significantly decreased with treatment (q = 0.003, 0.0003, and 0.005, respectively). There were several cytokines (*CCL5*, *CXCL11*, *IL1A*, *IL10*, and *IL12B*) that amplified in the TGF-β-only treatment group but did not amplify in the TGF-β + HPI-1 group, suggesting that treatment with HPI-1 substantially reduced expression of these genes as well (**Table S5**). HLA class I genes, *B2M* (β_2 macroglobulin, a component of HLA class I), and *CD274* (PD-L1) did not significantly change (Fig. 4**A**), suggesting that HPI-1 treatment may not impact direct tumor cell interactions with T cells through these mechanisms.

This experiment was also repeated in MDA-MB-436 cells, which showed similar patterns of altered cytokine expression in response to HPI-1 treatment (Fig. 5). While *PTHLH* did not significantly decrease, *GLI1* decreased with HPI-1 treatment, consistent with prior observations that Gli2 is upstream of Gli1 in TGF-β-mediated noncanonical Hedgehog signaling[47]. There were substantial overlaps in immune signaling-related genes modified by HPI-1 treatment in the MDA-MB-436 cells

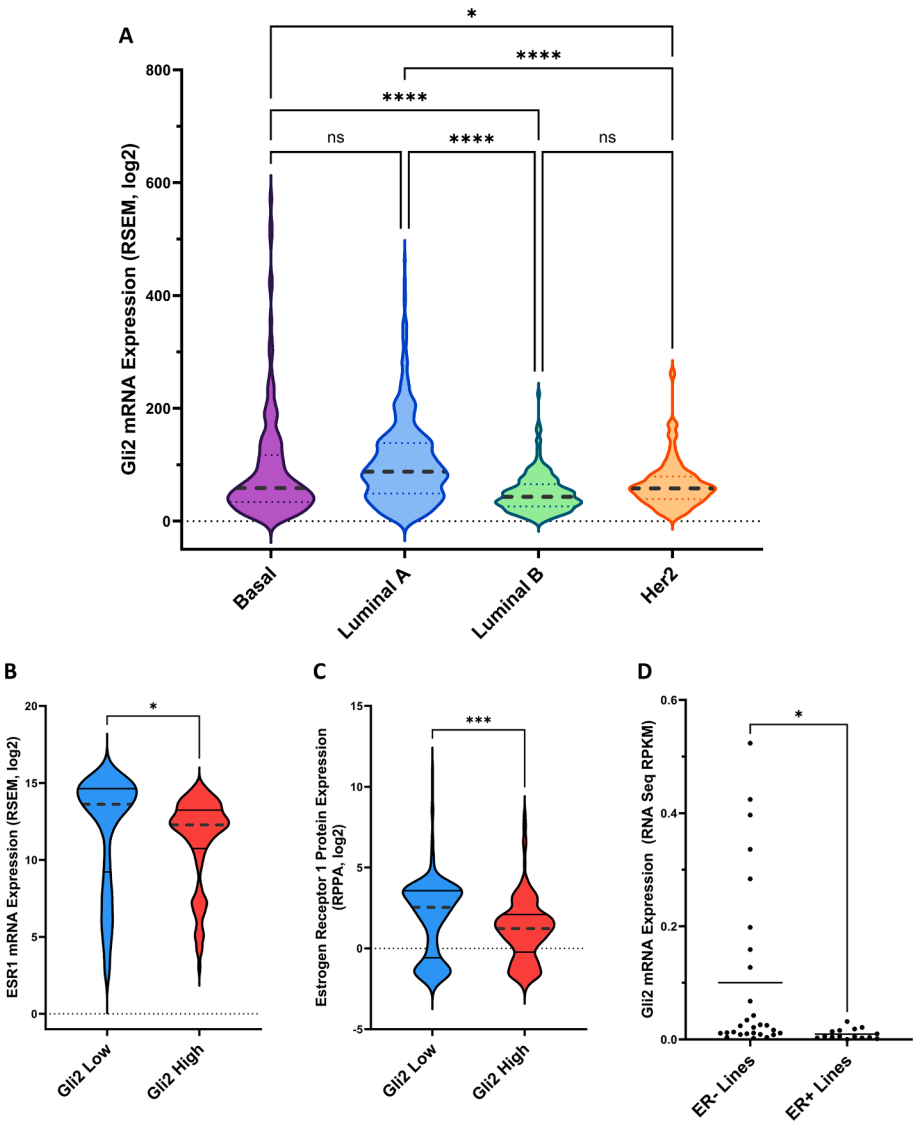

Fig. 3. Gli2 is expressed in all major breast cancer subtypes and has differential expression in cell lines. (A) Gli2 mRNA expression in basal (n = 171), luminal A (n = 499), luminal B (n = 197), and Her2 (n = 78) tumors in TCGA. The normal-like subtype was excluded from analysis. (B) and (C) show estrogen receptor 1 gene (ESR1) and protein expression, respectively, in tumors in the top and bottom quartiles of Gli2 expression (protein data available for 205 Gli2-high tumors and 223 Gli2-low tumors). Estrogen receptor expression is significantly higher in Gli2-low tumors. (D) Gli2 expression in estrogen receptor-negative and –positive cell lines in the Cancer Cell Line Encyclopedia was queried using cBioPortal, and outliers were omitted. ER-negative lines (n = 28) have significantly higher Gli2 expression than ER-positive lines (n = 15). Heavy dashed line in violin plots represents median. Solid line in (D) represents mean. *p < 0.05, ***p < 0.0005, ****p < . 0.0001.

compared to the MDA-MB-231b cells shown in (Fig. 4), such as decreases in *CCL2*, *IL6*, and *CSF1/CSF3*. Interestingly, there were numerous cytokine genes that were significantly changed in the treated MDA-MB-436 cells that did not change in the MDA-MB-231b cells (including several chemokines such as *CXCL10* and *CXCL11*) as well as some opposing changes (such as an increase in *TNF* expression in treated MDA-MB-231b cells and corresponding decrease in MDA-MB-436 cells). The remaining genes assayed from **Table S1** were not amplified in either group, except *CCL7*, *IL10*, *IL12B*, and *IL13*, which were expressed in the TGF-β-only group but not amplified in the TGF-β + HPI-1 group. Despite some potential differences in drug response between cell lines, this data demonstrates that inhibition of noncanonical Hedgehog signaling modifies gene expression of cytokines in osteolytic tumor cells, warranting further investigation of which cytokines may be mediating interactions between these breast cancer cells and myeloid populations.

3.3. Hedgehog pathway inhibitor treatment induces differential cytokine secretion by osteolytic breast cancer cells

We then sought to determine if transcriptional changes found in HPI-1-treated cells resulted in changes in their secreted cytokine profile. We first performed an enzyme-linked immunosorbent assay (ELISA) for CSF-1/M−CSF on conditioned media from TGF-β-stimulated MDA-MB-231b cells treated with or without 5 μM HPI-1. Protein secretion of macrophage colony stimulating factor (M−CSF/CSF-1), which was transcriptionally reduced by almost 70% as shown above, was significantly lower in HPI-1 treated cells (Fig. 6**A**). Then, the MILLIPLEX MAP Human Cytokine/Chemokine Magnetic Bead Panel was performed on the same conditioned media to evaluate presence of a subset cytokines from the genes assayed above (Fig. 6**B**). Surprisingly, there were several cytokines which were not detected in the conditioned media (G-CSF/CSF-3, IL-1α, IL-10, CCL5/RANTES, and TNF-α). However, several of the detected cytokines that accumulated in the conditioned media followed similar trends to those seen in the PCR arrays above, albeit with

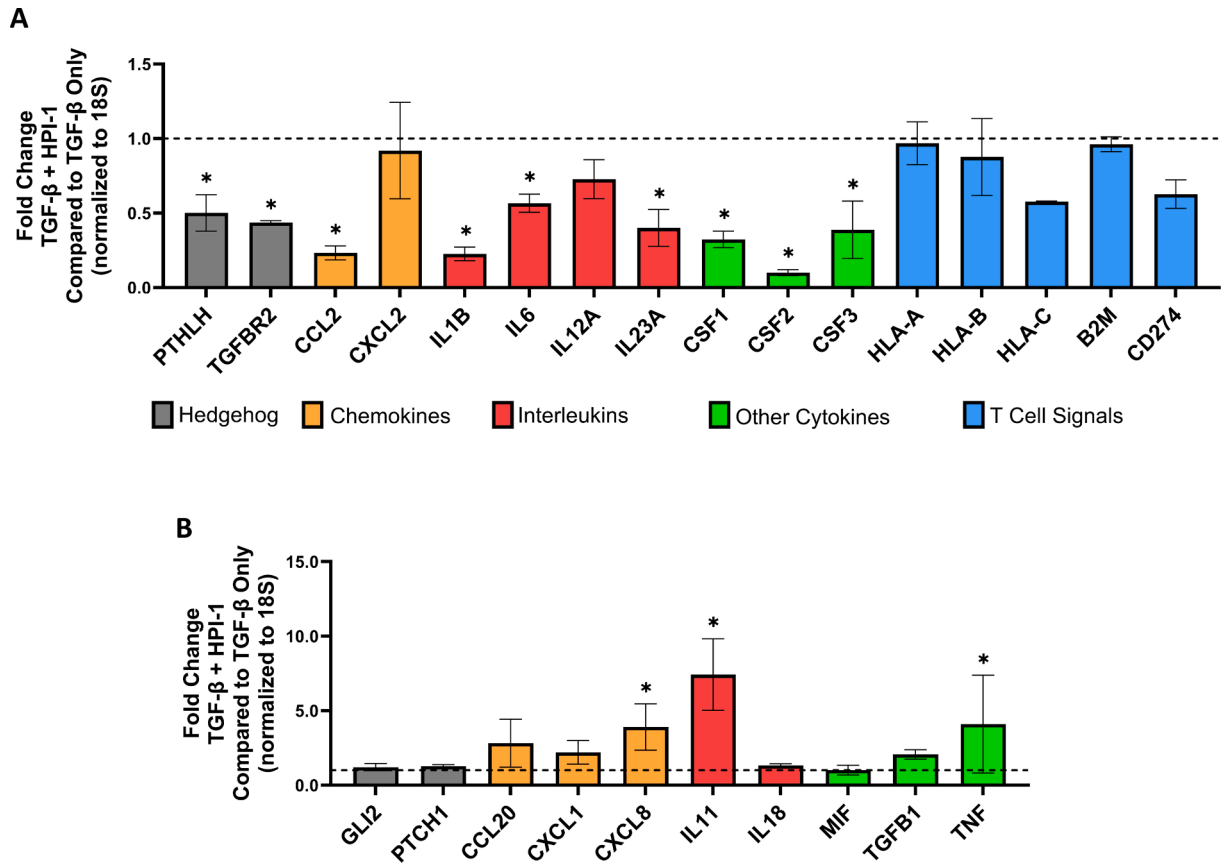

Fig. 4. HPI-1 treatment changes expression of key immune signaling-related genes in TGF-β-stimulated MDA-MB-231b breast cancer cells. In addition to decreasing genes important in Hedgehog activity of osteolytic breast cancer cells (PTHLH, TGFBR2), HPI-1 treatment alters expression of cytokines such as CCL2 and CSF1/2/3. (A) Genes with decreased expression in HPI-1-treated cells compared to TGF-β only (fold change < 1). (B) Genes with increased expression in HPI-1-treated cells (fold change > 1). Mean and standard deviation shown. *q < 0.05. Biological replicates from three independent experiments.

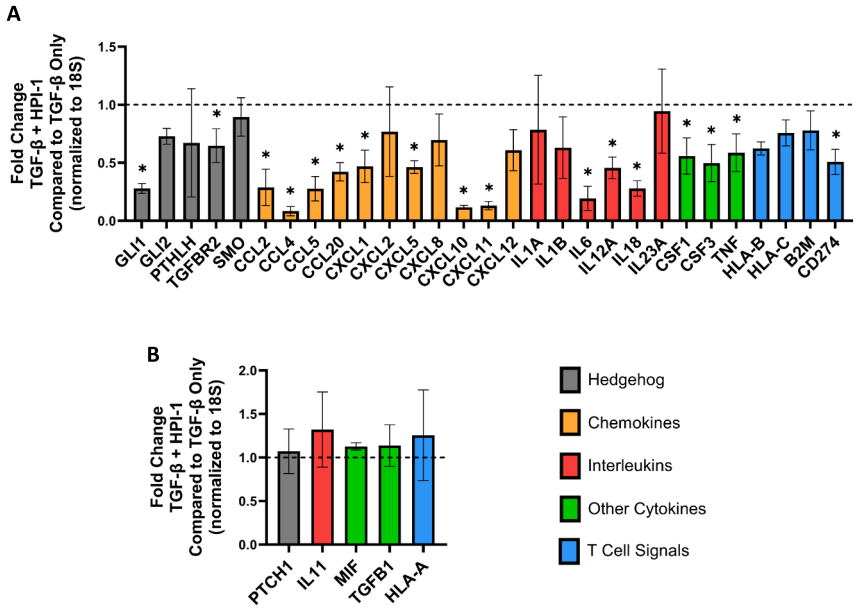

Fig. 5. HPI-1 treatment changes expression of key immune signaling-related genes in TGF-β-stimulated MDA-MB-436 breast cancer cells. While PTHLH does not significantly change in HPI-1 treated MDA-MB-436 cells, GLI1 and TGFBR2 decrease, as does the expression of numerous cytokines. (A) Genes with decreased expression in HPI-1-treated cells compared to TGF-β only (fold change < 1). (B) Genes with increased expression in HPI-1-treated cells (fold change > 1). Mean and standard deviation shown. *q < 0.05. Biological replicates from three independent experiments.

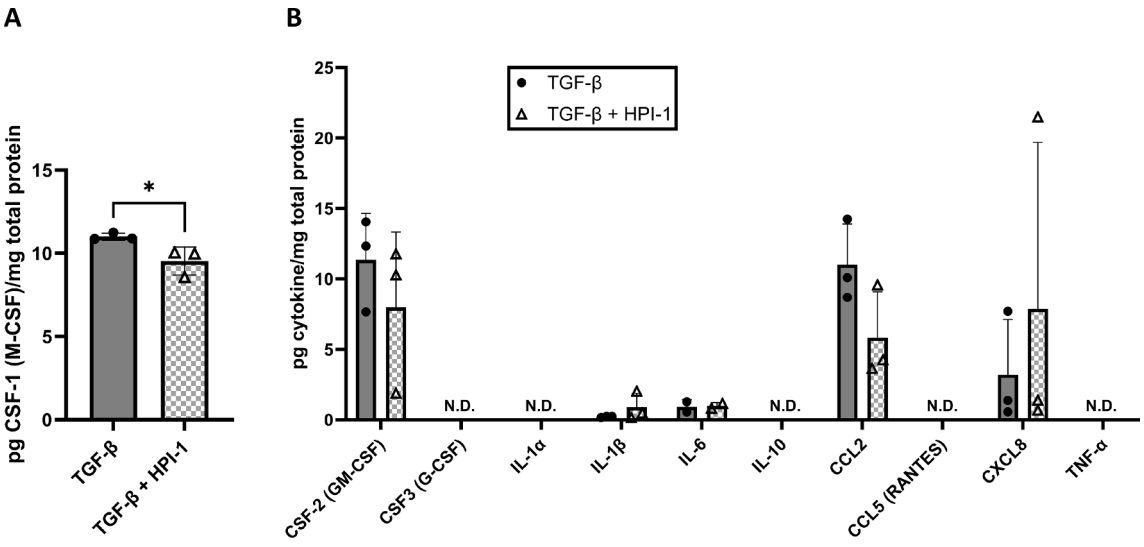

Fig. 6. HPI-1 treatment decreases M−CSF secretion in TGF-β-stimulated MDA-MB-231b breast cancer cells. (A) Conditioned media was collected from treated cells. ELISA demonstrates decreased M−CSF expression in HPI-1 treated cells. (B) MILLIPLEX MAP Human Cytokine/Chemokine Magnetic Bead Panel was performed on the same conditioned media using a subset of targets. Detected proteins show similar trends to transcriptional changes shown in Fig. 4. Mean and standard deviation shown. *p < 0.05. Biological replicates from three independent experiments. N.D. = not detected.

variability in some groups. The CSF-1/M−CSF ELISA was also performed on conditioned media from treated MDA-MB-436 cells, which showed similar trends to the MDA-MB-231b cells though not statistically significant (**Figure S2**).

These results reaffirm that noncanonical Hedgehog signaling inhibition affects the cytokine milieu from osteolytic breast cancer cells, particularly M−CSF. The link between noncanonical Hedgehog signaling and M−CSF/CSF-1 expression is further supported by publicly available patient tumor sequencing data. In addition to significant differences in CSF-1 and CSF-1R in Gli2 high versus low tumors in Fig. 2**C**, among primary tumor samples from patients with known bone metastasis in The Metastatic Breast Cancer Project[25–27,32], there were strong correlations between Gli2 gene expression and CSF1 and its receptor (Spearman's correlation 0.4482 and 0.3807, respectively) (**Figure S3A-B**).

3.4. Treatment with tumor-conditioned media from treated osteolytic breast cancer cells alters the phenotype of human monocytic cells

To determine if HPI-1 treatment-mediated cytokine changes affect tumor-myeloid cell interactions, THP-1 human monocytic cells were treated with conditioned media from pretreated tumor cells. Although MDA-MB-231b and MDA-MB-436 cells showed overlapping cytokine transcription responses to drug treatment, the change in M−CSF cytokine secretion was only significant in MDA-MB-231b cells (Fig. 6**A**). Furthermore, MDA-MB-436 cells have higher baseline Gli1 expression than MDA-MB-231 cells in gene expression data from the Cancer Cell Line Encyclopedia[34], suggesting that HPI-1 effects in MDA-MB-231b cells may be more Gli2-specific than that in MDA-MB-436 cells, particularly with the significant decrease in PTHLH in HPI-1 treated MDA-MB-231b cells (Fig. 4**A**) not seen in MDA-MB-436 cells (Fig. 5**A**). Therefore, subsequent experiments were only performed with MDA-MB-231b cells. Tumor cells were treated with TGF-β with or without 5 μM HPI-1 for 48 h. Drug treatment was then removed, and cells were cultured for 24 or 48 additional hours in serum-free media to allow cytokines to accumulate. Tumor-conditioned media collected 24 h after TGF-β or TGF-β + HPI-1 treatment cessation is called T24 pretreat TCM and TH24 pretreat TCM, respectively. Tumor-conditioned media collected 48 h after TGF-β or TGF-β + HPI-1 treatment cessation is called T48 pretreat TCM and TH48 pretreat TCM, respectively. These treatments are detailed in **Table S6**. This pretreated TCM was applied to THP-1 cells in a 1:1 ratio with complete RPMI for 72 h (**Figure S4A**). Cells were collected, and RNA was extracted using Qiazol. A small percentage of cells in all treatment groups were adherent, but the fraction was too small to obtain adequate sample to analyze adherent and nonadherent fractions separately, so all cells within each group were pooled. qRT-PCR analysis demonstrated that THP-1 cells treated with TH48 pretreat TCM had higher CD14 expression than cells treated with T48 pretreat TCM (**Figure S4B-C**). CD14 is a surface receptor that increases when THP-1 cells are pushed toward a pro-inflammatory phenotype upon PMA stimulation[48,49]. This suggests that although the other genes tested were not significantly changed, there may be myeloid population shifts occurring due to TCM treatment, which may be obscured by evaluating bulk RNA.

Based on this information, TCM treatment on THP-1 cells was then repeated for three and five days, and flow cytometry was performed for key myeloid phenotypic markers. There were no significant differences in cell count or viability between treatment groups (**Figure S5**). Live singlet cells were gated on CD45 to exclude any possible retained tumor cells in the TCM. There was a significant increase in CD14 expression at three days of treatment with TH48 pretreat TCM, as previously seen in via qRT-PCR. However, this effect was dampened after five days of TCM treatment (Fig. 7**A-C**). Because CD14 can be considered a marker of proinflammatory THP-1 polarization[48,49], we then evaluated the expression of the antigen-presenting cell surface receptor HLA-DR within the CD14+ population (Fig. 7**D-F**). At three and five days of treatment, there was no difference in HLA-DR expression between THP-1 cells treated with TH48 pretreat TCM and T48 pretreat TCM. However, there was a significant increase in CD40 expression within the HLA-DR+ cells in the TH48 pretreat TCM group after five days of treatment (Fig. 7**G-I**). These changes in surface marker expression are indicative of a more proinflammatory state in monocytes treated with TCM from HPI-1-pretreated tumor cells.

These effects were not observed in THP-1 cells treated with TCM from tumor cells 24 h after treatment cessation (T24 and TH24 pretreat TCM) (**Figure S6**). This suggests that the secreted factors from HPI-1-pretreated tumor cells must accumulate in the TCM in order to fully exert their effects on the THP-1 cells. Furthermore, we evaluated the expression of CD206, CD163, and PD-L1, all markers of an immunosuppressive myeloid phenotype, on CD45+ THP-1 cells (**Figure S7**). Cells were not gated on CD14 for this evaluation due to its role as a marker of a proinflammatory THP-1 cell phenotype[48,49]. After three

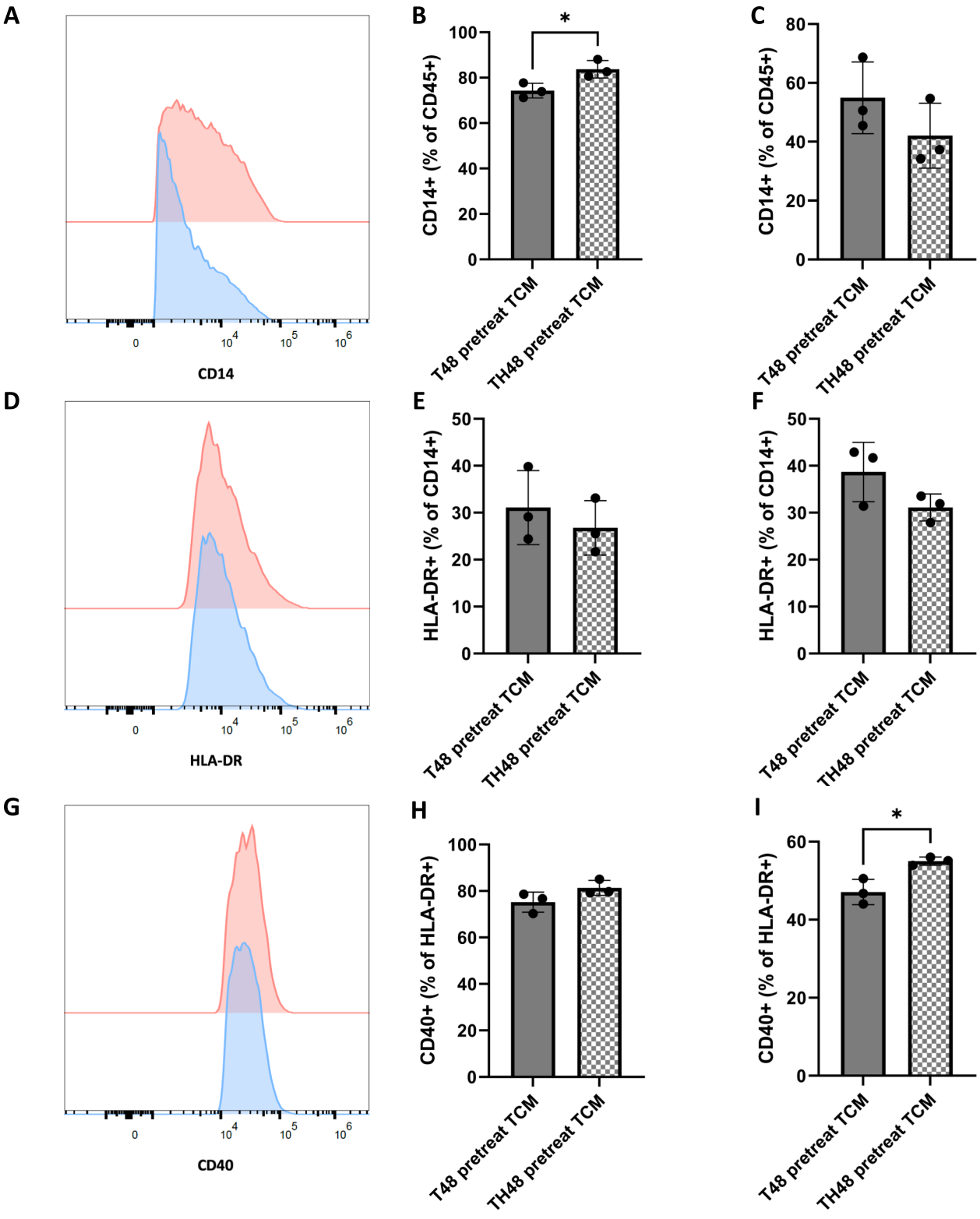

Fig. 7. Conditioned media from HPI-1-pretreated tumor cells increases proinflammatory markers on THP-1 monocytes. (A) Representative histogram of CD14 (CD45+) expression in THP-1 cells treated for three days with TCM: TH48 pretreat TCM (red) and T48 pretreat TCM (blue). Bar graphs shown for all biological replicates from (B) three and (C) five days of TCM treatment. (D) Representative histogram of HLA-DR (CD45+/CD14+) expression in THP-1 cells treated for three days (E: three days, F: five days). (G) Representative histogram of CD40 (CD45+/CD14+/HLA-DR+) expression in THP-1 cells treated for three days (H: three days, I: five days). *$p < 0.05$. Biological replicates from three independent experiments. (For interpretation of the references to colour in this figure legend, the reader is referred to the web version of this article.)

days of TCM treatment, there was no difference among treatment groups. Interestingly, after five days of treatment, cells positive for these immunosuppressive markers were too low to reliably measure across all treatment groups (data not shown).

Finally, the expression of Hedgehog signaling components within the THP-1 cells themselves was evaluated. Expression data of noncanonical and canonical Hedgehog signaling components in THP-1 cells versus the breast cancer cell lines used in this study was obtained from CCLE[34]. This data shows that THP-1 cells have low expression of the Gli protein-encoding genes as well as the downstream effector used by breast cancer cells in osteolytic disease, PTHLH. Of the major components of noncanonical Hedgehog signaling evaluated, only TGFBR2 is expressed by THP-1 cells in comparable amounts to the breast cancer lines (**Figure S8**). Therefore, although TGF-β stimulation may play a role in activating some signaling cascades in THP-1 cells, it is unlikely to activate noncanonical Hedgehog signaling, and THP-1 cells would not respond to HPI-1 treatment like the osteolytic breast cancer cells do. This is supported by data from the Human Protein Atlas showing that bone marrow and circulating immune cells do not have detectable Gli2 [31]. In total, these results demonstrate that the secretory profile of MDA-MB-231b cells can be altered by inhibition of noncanonical Hedgehog signaling, and these changes can support a proinflammatory phenotype in THP-1-derived monocytes.

4. Discussion and conclusions

Metastasis of breast cancer to bone has a deleterious effect on patient outcomes and quality of life. Despite great strides in treating the primary tumor over recent decades, cure for bone metastatic disease remains elusive due in part to complex interactions within the tumor microenvironment. One potential therapeutic avenue is targeting tumor-immune interactions to attenuate their tumor-supportive phenotype. Myeloid populations such as myeloid-derived suppressor cells and tumor-associated macrophages provide a key supportive role in the establishment and maintenance of bone metastases, and targeting them shows promise in reducing TIBD[22,24,50]. A better understanding of the mechanisms that promote these tumor-supportive myeloid populations can provide insight into improved treatment strategies.

Breast cancer bone metastatic tumors overexpress the transcription factor Gli2[9], which plays a key role in the significant bone deterioration characteristic of osteolytic disease[8,11]. Literature in a variety of disease states has identified methods by which Gli2 or Hedgehog signaling more broadly may affect immune populations, such as by altering cytokine expression[17–20], inducing PD-L1 expression [51,52], or affecting T cell receptor signaling[17,53]. These findings suggest that noncanonical Hedgehog signaling in bone metastatic breast cancer cells may play a similar role.

In this study, we sought to identify how inhibition of noncanonical Hedgehog signaling alters cytokine expression by osteolytic breast cancer cells and to explore how the phenotype of myeloid cells changes in response to this differential tumor cytokine secretion (working model in Fig. 8). First, we validated the clinical applicability of this question by analyzing the coexpression of Gli2 and key myeloid population markers in patient tumor data from TCGA (Figs. 1-2). We found that Gli2 is correlated with markers of myeloid lineage and phenotype, and Gli2-high tumors have a preponderance of markers of myeloid activity and differentiation compared to Gli2-low tumors. Furthermore, Gli2-high tumors had higher levels of numerous cytokines that can be involved in recruiting anti-inflammatory, tumor-supportive myeloid populations. These findings supported our goal of identifying how inhibition of noncanonical Hedgehog signaling in tumor cells may alter their cytokine profile.

Because Gli2 is overexpressed in bone metastatic tumors[9] and increases TIBD through its expression in the tumor cells themselves[11], we focused our studies on inhibiting noncanonical Hedgehog signaling *in vitro*. While Gli2 is expressed among the major breast cancer subtypes,

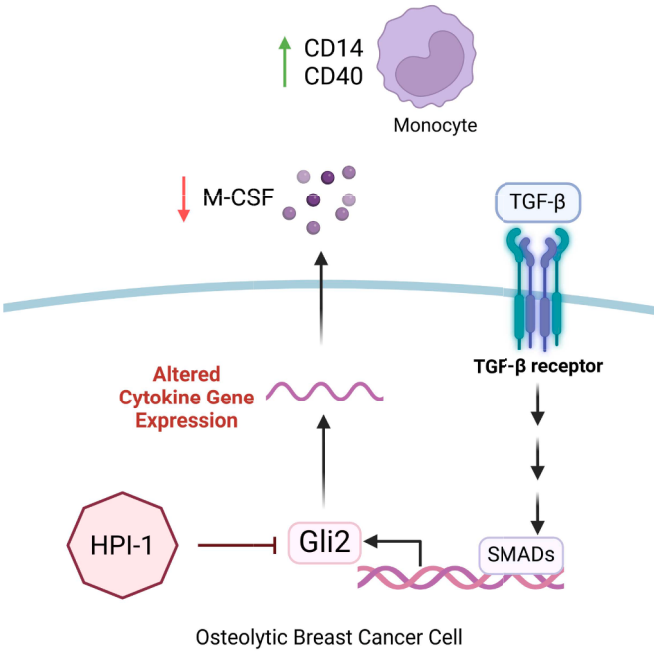

Fig. 8. Working model of the effect of noncanonical Hedgehog pathway inhibition on tumor cell cytokine expression and subsequent tumor-myeloid cell interactions. HPI-1 treatment inhibits TGF-β-stimulated Hedgehog signaling in osteolytic breast cancer cells, while simultaneously altering cytokine gene expression and secretion. This results in an increase in pro-inflammatory surface marker expression on monocytes. Schematic created with BioRender.com.

among Gli2-expressing cell lines, estrogen receptor-negative lines predominate (Fig. 3). Acknowledging this limitation of available cell lines, we proceeded with two triple-negative lines: a bone metastatic variant of the human breast cancer cell line MDA-MB-231 in addition to another known osteolytic breast cancer line, MDA-MB-436. Treatment with HPI-1 altered the expression of numerous cytokines, including several known to be involved in TIBD (Figs. 4-5). For example, CCL2 recruits monocytes to the bone metastatic site, where they become tumor-supporting macrophages[24], and Il-6 increases osteolysis by activating signaling cascades both in tumor cells and osteoblasts[54].

Among the most notable cytokine expression changes was the reduction in expression of the colony stimulating factors (*CSF1*, *2*, and *3*). CSF-1 (M−CSF) is of particular interest due to previous studies suggesting its importance in TIBD. In fact, the activities of CSF-1 and its receptor are known to be important in the differentiation and activity of osteoclasts[55,56], and blockade of this signaling axis reduces M2-like tumor-associated macrophages (TAMs) and osteoclast activity[57] as well as tumor burden[24,58]. In addition to a significant reduction of *CSF1* gene expression due to HPI-1 treatment, protein levels of this cytokine decreased in the conditioned media of treated MDA-MB-231b cells (Fig. 6). This further supports the hypothesis that inhibition of noncanonical Hedgehog signaling may alter the composition of cytokines released by tumor cells, thereby altering the ability of the tumor cells to induce tumor-supportive myeloid populations.

Finally, THP-1 human monocytes were treated with tumor-conditioned media from MDA-MB-231b cells pretreated with TGF-β with or without 5 μM HPI-1. Gene expression of the cell surface marker CD14 increased with HPI-1-pretreated TCM as measured by qRT-PCR, suggesting a potential phenotypic shift (Fig. 4). This was characterized in more detail by flow cytometry, which demonstrated that TCM from tumor cells pretreated with HPI-1 induced higher CD14 surface expression in THP-1 monocytes as well as an increase in CD40+ cells within the antigen-presenting HLA-DR+ population (Fig. 7).

Interestingly, the increase in CD14 occurred at an earlier timepoint (three days of TCM treatment), whereas the increase in CD40 occurred later (five days). This may reflect a trajectory along proinflammatory polarization, but other factors may be involved, such as increasing cell density over the course of treatment. This proinflammatory polarization of the THP-1 monocytes may be due to the reduction of M−CSF in the conditioned media of HPI-1-treated MDA-MB-231b cells. Although M−CSF is notable for recruiting monocytic populations to tumors and can induce maturation along the myeloid lineage, it also can result in an immunosuppressive phenotype in myeloid cells[59]. Work utilizing THP-1 cells specifically has shown that M−CSF alone is not sufficient to induce THP-1 maturation[60], and one study showed that M−CSF does not affect CD14 expression in THP-1 cells[61]. Therefore, in this model, we are utilizing CD14 as a marker of proinflammatory polarization in THP-1 cells alongside CD40. This phenotypic change may be in part due to reduced M−CSF in the conditioned media but can also be a result of alterations in secreted factors not explored in our current studies. Further studies can explore the role of HPI-1 on immunosuppressive surface markers, which were low in our experiments, to better understand this relationship. Infiltrating monocytes are the primary population from which bone metastasis-supporting macrophage populations originate[24], so the potential of noncanonical Hedgehog inhibition to polarize these populations toward a proinflammatory phenotype is promising.

In total, our results suggest that pharmacologic inhibition of noncanonical Hedgehog signaling in osteolytic breast cancer cells reduces expression and secretion of immunosuppressive cytokines such as M−CSF, and this altered secretory profile induces a proinflammatory myeloid phenotype in human monocytes. Our lab has previously shown that pharmacologic and genetic inhibition of this signaling pathway by targeting Gli2 is effective in reducing tumor cell proliferation and TIBD [9,50]. The results presented here suggest the potential value of investigating a therapeutic approach that can have direct anti-tumor effects but also influence the tumor immune microenvironment. There is also an opportunity for studying combination therapies, such as inhibition of the CSF-1/CSF-1R signaling axis, which has been shown to be effective in TIBD by reducing tumor-supportive myeloid populations, tumor burden, and bone destruction[57,58,62]. In fact, CSF-1 has been identified as a downstream target of Gli1 in pancreatic tissue repair[63], and our work is the first to our knowledge to link Gli2 or noncanonical Hedgehog signaling to CSF-1 expression in the context of breast cancer.

We acknowledge that altering tumor-myeloid interactions via Hedgehog inhibition does not occur in a vacuum, and these findings may have broader effects in the tumor microenvironment due to the pleiotropic roles of cytokines in recruiting and differentiating other immune populations. Finally, while this study centered around osteolytic breast cancer cells, these findings may be applicable to other Hedgehog-driven cancers.

CRediT authorship contribution statement

Natalie E. Bennett: Conceptualization, Methodology, Validation, Investigation, Writing – original draft, Writing – review & editing, Visualization. **Dominique V. Parker**: Methodology, Investigation, Writing – review & editing. **Rachel S. Mangano**: Investigation, Writing – review & editing. **Jennifer E. Baum**: Investigation, Writing – review & editing. **Logan A. Northcutt**: Investigation, Writing – review & editing. **Jade S. Miller**: Investigation, Writing – review & editing. **Erik P. Beadle**: Investigation, Writing – review & editing. **Julie A. Rhoades**: Conceptualization, Resources, Writing – review & editing, Supervision, Funding acquisition.

Declaration of competing interest

The authors declare that they have no known competing financial interests or personal relationships that could have appeared to influence the work reported in this paper.

Acknowledgements

Luminex assays were performed by the VUMC Hormone Assay and Analytical Services Core which is supported by NIH grants DK059637 and DK020593. The authors also thank Dr. Christian Warren in the flow cytometry core at the United States Department of Veterans Affairs, Tennessee Valley Healthcare System, Nashville, TN for his assistance with flow cytometry experiments.

This work was supported by the Veterans Health Administration under grant number 5I01BX001957 and the National Institutes of Health under award numbers 1R01CA264508 and T32GM007347. The content is solely the responsibility of the authors and does not necessarily represent the official views of the National Institutes of Health.

The results shown here are in part based upon data generated by the TCGA Research Network: https://www.cancer.gov/tcga. Additionally, the results included here include the use of data from The Metastatic Breast Cancer Project (https://www.mbcproject.org/), a project of Count Me In (https://joincountmein.org/) [32,33]. BioRender schematics were generated under the Vanderbilt University Medical Center plan with publishing rights.

Appendix A. Supplementary data

Supplementary data to this article can be found online at https://doi.org/10.1016/j.jbo.2024.100625.

References

[1] L. Gallicchio, T.P. Devasia, E. Tonorezos, M.A. Mollica, A. Mariotto, Estimation of the Number of Individuals Living With Metastatic Cancer in the United States, JNCI: Journal of the National Cancer Institute. 114 (11) (2022) 1476–1483, https://doi.org/10.1093/JNCI/DJAC158.

[2] H. Kennecke, R. Yerushalmi, R. Woods, et al., Metastatic behavior of breast cancer subtypes, Journal of Clinical Oncology. 28 (20) (2010) 3271–3277, https://doi.org/10.1200/JCO.2009.25.9820.

[3] R.K. Hernandez, S.W. Wade, A. Reich, M. Pirolli, A. Liede, G.H. Lyman, Incidence of bone metastases in patients with solid tumors: analysis of oncology electronic medical records in the United States, BMC Cancer. 18 (1) (2018) 44, https://doi.org/10.1186/s12885-017-3922-0.

[4] E. Terpos, C.B. Confavreux, P. Clézardin, Bone antiresorptive agents in the treatment of bone metastases associated with solid tumours or multiple myeloma, Bonekey Rep. 4 (2015) 744, https://doi.org/10.1038/BONEKEY.2015.113.

[5] C. Pulido, I. Vendrell, A.R. Ferreira, et al., Bone metastasis risk factors in breast cancer, Ecancermedicalscience. 11 (2017), https://doi.org/10.3332/ecancer.2017.715.

[6] R.E. Coleman, Clinical features of metastatic bone disease and risk of skeletal morbidity, Clinical Cancer Research. 12 (20) (2006) 6243s–6249s, https://doi.org/10.1158/1078-0432.CCR-06-0931.

[7] M.H. Wong, N. Pavlakis, Optimal management of bone metastases in breast cancer patients, Breast Cancer: Targets and Therapy. 3 (2011) 35–60, https://doi.org/10.2147/BCTT.S6655.

[8] J.A. Sterling, B.O. Oyajobi, B. Grubbs, et al., The Hedgehog signaling molecule Gli2 induces parathyroid hormone-related peptide expression and osteolysis in metastatic human breast cancer cells, Cancer Res. 66 (15) (2006) 7548–7553, https://doi.org/10.1158/0008-5472.CAN-06-0452.

[9] J.P. Vanderburgh, K.A. Kwakwa, T.A. Werfel, et al., Systemic delivery of a Gli inhibitor via polymeric nanocarriers inhibits tumor-induced bone disease, Journal of Controlled Release. 311–312 (2019) 257–272, https://doi.org/10.1016/j.jconrel.2019.08.038.

[10] S.A. Cannonier, J.A. Sterling, The role of hedgehog signaling in tumor induced bone disease, Cancers (basel). 7 (3) (2015) 1658–1683, https://doi.org/10.3390/cancers7030856.

[11] R.W. Johnson, M.P. Nguyen, S.S. Padalecki, et al., TGF-β promotion of Gli2-induced expression of parathyroid hormone-related protein, an important osteolytic factor in bone metastasis, is independent of canonical Hedgehog signaling, Cancer Res. 71 (3) (2011) 822–831, https://doi.org/10.1158/0008-5472.CAN-10-2993.

[12] J. Xu, S. Acharya, O. Sahin, et al., 14–3-3ζ Turns TGF-β's Function from Tumor Suppressor to Metastasis Promoter in Breast Cancer by Contextual Changes of Smad Partners from p53 to Gli2, Cancer Cell. 27 (2) (2015) 177–192, https://doi.org/10.1016/J.CCELL.2014.11.025.

[13] de Reyniès A, Javelaud D, Elarouci N, Marsaud V, Gilbert C, Mauviel A. Large-scale pan-cancer analysis reveals broad prognostic association between TGF-β ligands, not Hedgehog, and GLI1/2 expression in tumors. *Scientific Reports 2020 10:1*. 2020; 10(1):1-8. doi:10.1038/s41598-020-71559-w.

[14] S. Dennler, J. André, F. Verrechia, A. Mauviel, Cloning of the Human GLI2 Promoter, J Biol Chem. 284 (46) (2009) 31523, https://doi.org/10.1074/JBC.M109.059964.

[15] S.A. Cannonier, C.B. Gonzales, K. Ely, S.A. Guelcher, J.A. Sterling, Hedgehog and TGFβ signaling converge on Gli2 to control bony invasion and bone destruction in oral squamous cell carcinoma, Oncotarget. 7 (46) (2016) 76062–76075, https://doi.org/10.18632/oncotarget.12584.

[16] J. Vanderburgh, J.L. Hill, M.K. Gupta, et al., Tuning Ligand Density to Optimize Pharmacokinetics of Targeted Nanoparticles for Dual Protection against Tumor-Induced Bone Destruction, ACS Nano. 14 (1) (2020) 311–327, https://doi.org/10.1021/acsnano.9b04571.

[17] A.L. Furmanski, J.I. Saldana, M. Ono, et al., Tissue-Derived Hedgehog Proteins Modulate Th Differentiation and Disease, The Journal of Immunology. 190 (6) (2013) 2641–2649, https://doi.org/10.4049/jimmunol.1202541.

[18] E. Papaioannou, D.C. Yánez, S. Ross, et al., Sonic Hedgehog signaling limits atopic dermatitis via Gli2-driven immune regulation, Journal of Clinical Investigation. 129 (8) (2019) 3153–3170, https://doi.org/10.1172/JCI125170.

[19] Z. Liu, K. Lai, Y. Xie, X. He, X. Zhou, Gli2 Mediated Activation of Hedgehog Signaling Attenuates Acute Pancreatitis via Balancing Inflammatory Cytokines in Mice, Cellular Physiology and Biochemistry. 48 (1) (2018) 120–130, https://doi.org/10.1159/000491668.

[20] S.F. Elsawa, L.L. Almada, S.C. Ziesmer, et al., GLI2 transcription factor mediates cytokine cross-talk in the tumor microenvironment, Journal of Biological Chemistry. 286 (24) (2011) 21524–21534, https://doi.org/10.1074/jbc.M111.234146.

[21] M.K. Scales, A. Velez-Delgado, N.G. Steele, et al., Combinatorial Gli activity directs immune infiltration and tumor growth in pancreatic cancer, PLoS Genet. 18 (7) (2022) e1010315.

[22] S. Danilin, A.R. Merkel, J.R. Johnson, R.W. Johnson, J.R. Edwards, J.A. Sterling, Myeloid-derived suppressor cells expand during breast cancer progression and promote tumor-induced bone destruction, Oncoimmunology. 1 (9) (2012) 1484–1494, https://doi.org/10.4161/onci.21990.

[23] L. Monteran, N. Ershaid, I. Sabah, et al., Bone metastasis is associated with acquisition of mesenchymal phenotype and immune suppression in a model of spontaneous breast cancer metastasis, Sci Rep. 10 (1) (2020) 1–14, https://doi.org/10.1038/s41598-020-70788-3.

[24] R.Y. Ma, H. Zhang, X.F. Li, et al., Monocyte-derived macrophages promote breast cancer bone metastasis outgrowth, Journal of Experimental Medicine. 217 (11) (2020), https://doi.org/10.1084/JEM.20191820.

[25] I. de Bruijn, R. Kundra, B. Mastrogiacomo, et al., Analysis and Visualization of Longitudinal Genomic and Clinical Data from the AACR Project GENIE Biopharma Collaborative in cBioPortal, Cancer Res. 83 (23) (2023) 3861, https://doi.org/10.1158/0008-5472.CAN-23-0816.

[26] Gao J, Aksoy BA, Dogrusoz U, et al. Integrative Analysis of Complex Cancer Genomics and Clinical Profiles Using the cBioPortal. *Sci Signal*. 2013;6(269):pl1. doi:10.1126/SCISIGNAL.2004088.

[27] E. Cerami, J. Gao, U. Dogrusoz, et al., The cBio Cancer Genomics Portal: An Open Platform for Exploring Multidimensional Cancer Genomics Data, Cancer Discov. 2 (5) (2012) 401, https://doi.org/10.1158/2159-8290.CD-12-0095.

[28] S. Carbon, A. Ireland, C.J. Mungall, et al., AmiGO: online access to ontology and annotation data, Bioinformatics. 25 (2) (2009) 288–289, https://doi.org/10.1093/bioinformatics/btn615.

[29] S.A. Aleksander, J. Balhoff, S. Carbon, et al., The Gene Ontology knowledgebase in 2023, Genetics. 224 (1) (2023), https://doi.org/10.1093/GENETICS/IYAD031.

[30] M. Ashburner, C.A. Ball, J.A. Blake, et al., Gene Ontology: tool for the unification of biology, Nat Genet. 25 (1) (2000) 25, https://doi.org/10.1038/75556.

[31] M. Karlsson, C. Zhang, L. Méar, et al., A single–cell type transcriptomics map of human tissues, Sci Adv. 7 (31) (2021), https://doi.org/10.1093/bioinformatics/btn615.

[32] Jain E, Gómez J, Zañudo T, et al. The Metastatic Breast Cancer Project: leveraging patient-partnered research to expand the clinical and genomic landscape of metastatic breast cancer and accelerate discoveries. *medRxiv*. Published online June 10, 2023:2023.06.07.23291117. doi:10.1101/2023.06.07.23291117.

[33] Wagle N, Painter C, Krevalin M, et al. The Metastatic Breast Cancer Project: A national direct-to-patient initiative to accelerate genomics research. *Journal of Clinical Oncology*. 2016;34(18_suppl):LBA1519-LBA1519. doi:10.1200/JCO.2016.34.18_SUPPL.LBA1519.

[34] M. Ghandi, F.W. Huang, J. Jané-Valbuena, et al., Next-generation characterization of the Cancer Cell Line Encyclopedia, Nature. 569 (7757) (2019) 503–508, https://doi.org/10.1038/S41586-019-1186-3.

[35] L.E. Wright, P.D. Ottewell, N. Rucci, et al., Murine models of breast cancer bone metastasis, Bonekey Rep. 5 (2016) 804, https://doi.org/10.1038/BONEKEY.2016.31.

[36] R.W. Johnson, A.R. Merkel, J.M. Page, N.S. Ruppender, S.A. Guelcher, J. A. Sterling, Wnt signaling induces gene expression of factors associated with bone destruction in lung and breast cancer, Clin Exp Metastasis. 31 (8) (2014) 945–959, https://doi.org/10.1007/s10585-014-9682-1.

[37] Y. Kang, P.M. Siegel, W. Shu, et al., A multigenic program mediating breast cancer metastasis to bone, Cancer Cell. 3 (6) (2003) 537–549, https://doi.org/10.1016/S1535-6108(03)00132-6.

[38] Gionfriddo G, Plastina P, Augimeri G, et al. Modulating Tumor-Associated Macrophage Polarization by Synthetic and Natural PPARγ Ligands as a Potential Target in Breast Cancer. *Cells 2020, Vol 9, Page 174*. 2020;9(1):174. doi:10.3390/CELLS9010174.

[39] K. Sawa-Wejksza, A. Dudek, M. Lemieszek, K. Kaławaj, M. Kandefer-Szerszeń, Colon cancer–derived conditioned medium induces differentiation of THP-1 monocytes into a mixed population of M1/M2 cells, Tumor Biology. 40 (9) (2018), https://doi.org/10.1177/1010428318797880.

[40] A. Giammona, E. Crivaro, B. Stecca, Emerging Roles of Hedgehog Signaling in Cancer Immunity, Int J Mol Sci. 24 (2) (2023), https://doi.org/10.3390/IJMS24021321.

[41] X. Cheng, Z. Wang, Immune Modulation of Metastatic Niche Formation in the Bone, Front Immunol. 12 (2021) 765994, https://doi.org/10.3389/FIMMU.2021.765994/BIBTEX.

[42] S.J. Coniglio, Role of Tumor-Derived Chemokines in Osteolytic Bone Metastasis, Front Endocrinol (lausanne) 9(JUN):313 (2018), https://doi.org/10.3389/FENDO.2018.00313.

[43] M. Patysheva, I. Larionova, M. Stakheyeva, et al., Effect of Early-Stage Human Breast Carcinoma on Monocyte Programming. *Front*, Oncol. (2022) 11, https://doi.org/10.3389/FONC.2021.800235/FULL.

[44] J.M. Hyman, A.J. Firestone, V.M. Heine, et al., Small-molecule inhibitors reveal multiple strategies for Hedgehog pathway blockade, Proc Natl Acad Sci U S a. 106 (33) (2009) 14132–14137, https://doi.org/10.1073/pnas.0907134106.

[45] T. Trivedi, G.M. Pagnotti, T.A. Guise, K.S. Mohammad, The Role of TGF-β in Bone Metastases, Biomolecules. 11 (11) (2021), https://doi.org/10.3390/BIOM11111643.

[46] H.O. Oladapo, M. Tarpley, S.J. Sauer, et al., Pharmacological targeting of GLI1 inhibits proliferation, tumor emboli formation and in vivo tumor growth of inflammatory breast cancer cells, Cancer Lett. 411 (2017) 136, https://doi.org/10.1016/J.CANLET.2017.09.033.

[47] S. Dennler, J. André, I. Alexaki, et al., Induction of Sonic Hedgehog Mediators by Transforming Growth Factor-β: Smad3-Dependent Activation of Gli2 and Gli1 Expression In vitro and In vivo, Cancer Res. 67 (14) (2007) 6981–6986, https://doi.org/10.1158/0008-5472.CAN-07-0491.

[48] G. Jimenez-Duran, R. Luque-Martin, M. Patel, et al., Pharmacological validation of targets regulating CD14 during macrophage differentiation, EBioMedicine. 61 (2020) 103039, https://doi.org/10.1016/J.EBIOM.2020.103039.

[49] T. Liu, T. Huang, J. Li, et al., Optimization of differentiation and transcriptomic profile of THP-1 cells into macrophage by PMA, PLoS One. 18 (7) (2023) e0286056.

[50] D. Buenrostro, K.A. Kwakwa, N.E. Putnam, et al., Early TGF-β inhibition in mice reduces the incidence of breast cancer induced bone disease in a myeloid dependent manner, Bone. 113 (2018) 77–88, https://doi.org/10.1016/j.bone.2018.05.008.

[51] V. Koh, J. Chakrabarti, M. Torvund, et al., Hedgehog transcriptional effector GLI mediates mTOR-Induced PD-L1 expression in gastric cancer organoids, Cancer Lett. 518 (2021) 59–71, https://doi.org/10.1016/j.canlet.2021.06.007.

[52] J. Chakrabarti, L. Holokai, L.J. Syu, et al., Hedgehog signaling induces PD-L1 expression and tumor cell proliferation in gastric cancer, Oncotarget. 9 (100) (2018) 37439, https://doi.org/10.18632/ONCOTARGET.26473.

[53] A.L. Furmanski, A. Barbarulo, A. Solanki, et al., The transcriptional activator Gli2 modulates T-cell receptor signalling through attenuation of AP-1 and NFκB activity, J Cell Sci. 128 (11) (2015) 2085–2095, https://doi.org/10.1242/jcs.165803.

[54] T. Ara, Y.A. DeClerck, Interleukin-6 in Bone Metastasis and Cancer Progression, Eur J Cancer. 46 (7) (2010) 1223, https://doi.org/10.1016/J.EJCA.2010.02.026.

[55] X.M. Dai, G.R. Ryan, A.J. Hapel, et al., Targeted disruption of the mouse colony-stimulating factor 1 receptor gene results in osteopetrosis, mononuclear phagocyte deficiency, increased primitive progenitor cell frequencies, and reproductive defects, Blood. 99 (1) (2002) 111–120, https://doi.org/10.1182/blood.V99.1.111.

[56] K. Yagiz, S.R. Rittling, Both cell-surface and secreted CSF-1 expressed by tumor cells metastatic to bone can contribute to osteoclast activation, Exp Cell Res. 315 (14) (2009) 2442–2452, https://doi.org/10.1016/j.yexcr.2009.05.002.

[57] L. Fend, N. Accart, J. Kintz, et al., Therapeutic Effects of Anti-CD115 Monoclonal Antibody in Mouse Cancer Models through Dual Inhibition of Tumor-Associated Macrophages and Osteoclasts, PLoS One. 8 (9) (2013) 73310, https://doi.org/10.1371/journal.pone.0073310.

[58] J.Y. Hung, D. Horn, K. Woodruff, et al., Colony-stimulating factor 1 potentiates lung cancer bone metastasis, Laboratory Investigation. 94 (4) (2014) 371–381, https://doi.org/10.1038/labinvest.2014.1.

[59] D.A. Hume, K.P.A. MacDonald, Therapeutic applications of macrophage colony-stimulating factor-1 (CSF-1) and antagonists of CSF-1 receptor (CSF-1R) signaling, Blood. 119 (8) (2012) 1810–1820, https://doi.org/10.1182/BLOOD-2011-09-379214.

[60] C.R. Nascimento, N.A. Rodrigues Fernandes, L.A. Gonzalez Maldonado, J.C. Rossa, Comparison of monocytic cell lines U937 and THP-1 as macrophage models for in vitro studies, Biochem Biophys Rep. 32 (2022) 101383, https://doi.org/10.1016/J.BBREP.2022.101383.

[61] P.B. Aldo, V. Craveiro, S. Guller, G. Mor, Effect of culture conditions on the phenotype of THP-1 monocyte cell line, Am J Reprod Immunol. 70 (1) (2013) 80, https://doi.org/10.1111/AJI.12129.

[62] C. Liverani, L. Mercatali, C. Spadazzi, et al., CSF-1 blockade impairs breast cancer osteoclastogenic potential in co-culture systems, Bone. 66 (2014) 214–222, https://doi.org/10.1016/j.bone.2014.06.017.

[63] E. Mathew, M.A. Collins, M.G. Fernandez-Barrena, et al., The Transcription Factor GLI1 Modulates the Inflammatory Response during Pancreatic Tissue Remodeling, J Biol Chem. 289 (40) (2014) 27727, https://doi.org/10.1074/JBC.M114.556563.